2021 60th IEEE Conference on Decision and Control (CDC)
December 13-15, 2021. Austin, Texas

Disease spread coupled with evolutionary social distancing dynamics can lead to growing oscillations

Hossein Khazaei, Keith Paarporn, Alfredo Garcia, and Ceyhun Eksin

2021 60th IEEE Conference on Decision and Control (CDC) | 978-1-6654-3659-5/21/$31.00 ©2021 IEEE | DOI: 10.1109/CDC45484.2021.9683594

***Abstract*— If the public's adherence to social distance measures remained steady during an outbreak, the number of cases would have a single peak followed by a sharp decline according to standard epidemiological models. Nonetheless, during COVID-19 the initial rise and fall in the number of cases followed new waves of cases in many localities. In this paper, we explore a standard susceptible-exposed-infected-recovered (SEIR) epidemiological model coupled with an individual behavior response model that modulates the contact rate. A game with payoffs determined by the state of the disease captures the public's incentive to comply with the social distancing measures. We use replicator dynamics to model the response to changes in incentives. Using SEIR dynamics coupled with replicator dynamics, we identify a set of dynamics that can lead to growing oscillations in the number of cases until herd immunity is reached. According to the dynamics, an increase in the number of infected individuals changes the payoffs such that the public's cooperation level eventually increases. Increased cooperation levels is followed by a reduced number of cases in the community, which then reduces the public's incentive to cooperate. The decrease in the cooperation levels causes the number of cases to rise again. These waves correspond to cycles between cooperation and defection behavior, and the rise and fall of the number of the infected individuals. The proposed model also provides a proper tool to study the effects of the public health policies that aim to curb the growth in number of cases by providing incentives to cooperate.**

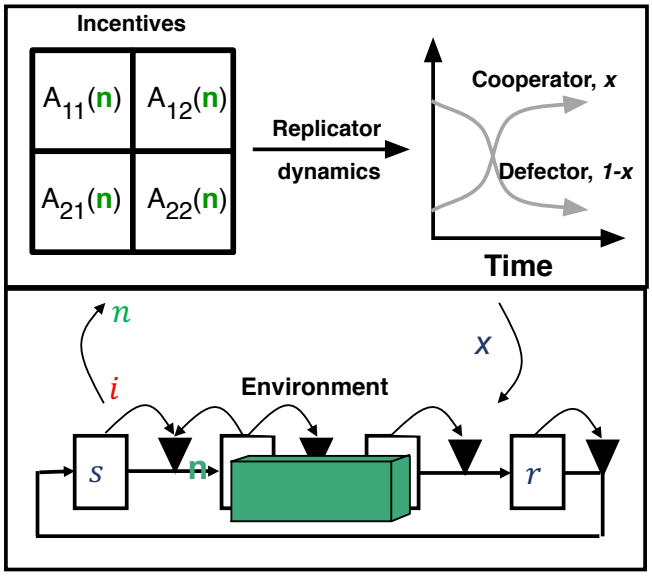

Fig. 1. An SEIRS model coupled with evolutionary behavior feedback. (Top) Cooperation with social distancing measures depend on the game payoffs and replicator dynamics. (Bottom) Cooperation level of the population (x) determines the transmission rate in the SEIRS dynamics. The payoff parameters depend on the current ratio of infected (i) through the environment state (n).

I. Introduction

Peak-centered paradigm spurred by Farr's law [1] and conventional compartmental epidemic models for emergent infectious diseases became obsolete during the COVID-19 outbreak where many localities experienced multiple peaks with subsequent peaks larger than the initial one. These observations have brought focus on the role of public behavior. Indeed, recommended public health polices and public's compliance with these measures have evolved over time, as indicated by Google mobility data and documented by recent studies [2], during the pandemic. These changes in behaviors and multiple peaks observed elicit further investigation into the relation between behavior changes and disease spread dynamics.

Standard epidemic models represent individuals in compartments according to the state of the disease they are in, e.g., susceptible, exposed, infected, recovered [3]–[5]. According to these models, if the inherent transmission rate of the disease is faster than the healing rate, the disease would grow exponentially in a predominantly susceptible population until a certain fraction of the individuals become immune, i.e., until *herd immunity* is reached. After herd immunity, some individuals would still get infected but the number of daily cases would begin to decrease exponentially. These models lead to a 'single-peak' in theory.

Public's willingness to cooperate with the recommended public health measures, i.e., social distance, has direct effects on the disease spread and depends on the risk perception of the disease [6], [7]. If enough people cooperate, then the disease can go to a decline phase before herd immunity is reached. This decline in the number of cases can reduce the incentive to comply with the public health recommendations. In such a setting, a drop in cooperation with the public health measures can lead to resurgence of the disease in the population.

In this paper, we propose a mechanistic model for public's cooperation with the recommended measures that is coupled with the disease prevalence. The cooperation level of the population evolves according to replicator dynamics, in which the frequency of cooperators in the society increases if the

H. Khazaei, A. Garcia and C. Eksin are with the Industrial and Systems Engineering Department, Texas A&M University, College Station, TX 77843. K. Paarporn is with the Electrical and Computer Engineering Department, University of California, Santa Barbara. E-mail: h.khazaei@tamu.edu; kpaarporn@ucsb.edu; alfredo.garcia@tamu.edu; eksinc@tamu.edu. This work was supported by NSF ECCS-1953694. Code is available on https://github.com/hoseinkh/CovidModel-CDC.

benefit of the cooperation is larger than defection (not taking the public health measures). The payoff from cooperating depend on the public's current cooperation level and the disease prevalence, i.e., a function of the number of cases. We consider payoffs such that defection is the dominant strategy when the environment is good, i.e., disease-free. As the disease prevalence increases, i.e., as the environment becomes risky, payoffs change such that cooperation is preferred—see Figure 1(Top).

We model the disease progression in the society using an SEIRS model where the flow from susceptible to an infected state is proportional to the product of fraction of individuals in susceptible and infected states [8]. The frequency of cooperators in the society regulate this flow. In addition, we consider loss of immunity, that is recovered individuals may transition back to being susceptible after some time—see Figure 1(Bottom).

We identify the disease free and endemic equilibria of the evolutionary social distancing model with disease feedback and study their stability properties. In particular, we find that in the endemic equilibrium in which a positive fraction of the population cooperates, the endemic disease level depends on how fast the payoffs change as a function of the number of cases. When the society is more responsive to changes in the number of cases, the number of cases is lower at the endemic equilibrium. In characterizing the disease and behavior trajectories for general payoff matrices, we identify growing surges until herd immunity is reached in settings where the selection strength for cooperators is strong when the disease prevalence is high. This behavior, recently documented in evolutionary games with environmental feedback [9], [10], is termed as the *oscillating tragedy of the commons* stemming from Hardin's *tragedy of the commons* in populations driven by selfish interests [11]. We also identify that the total outbreak size tends to decrease as the sensitivity of the public to changes in the case counts increases.

In our model we use social distancing behavior in general terms to refer to any behavior that aims to limit the risk of an interaction, e.g., wearing masks, standing 6ft. apart etc, similar to some of the earlier epidemic models that incorporate individual behavior response [12]–[21]. Some of the recent compartmental disease spread models that incorporate behavior response, e.g., [17], [19], showed that behavior changes can drive the epidemics toward exhibiting oscillations and plateaus. Similar to the model proposed here, an evolutionary dynamics driven behavior coupled with disease spread dynamics is proposed in [19], [21], [22]. These models, similar to the one proposed here, can exhibit diminishing or growing oscillations until herd immunity. Our contribution involves a characterization of all possible dynamics that can arise based on the set of all possible payoff values (games). In addition, we provide a characterization of the stability of the disease free state, and identify endemic equilibria in which endemic disease level is modulated by the public's cooperation level. The evolutionary game-theoretic modeling framework is amenable to any compartmental epidemic model, not just SEIR, and thus can be relevant in modeling other infectious disease outbreaks. Lastly, the model can be used to estimate population's perception of the costs and benefits of social distancing measures using publicly available data, e.g., hospitalization counts, which then can be used to forecast the disease trajectory or can aid in designing public health communication campaigns.

II. Evolutionary social distancing with disease feedback in an SEIRS model

We consider an SEIR model with loss of immunity, i.e., an SEIRS model, where upon contracting the disease from an infectious individual, the susceptible (s) individuals transition to exposed (e), infected (i), recovered (r) and then back to susceptible state due to loss of immunity, respectively—see Fig 1. We use s, e, i, and r to represent the fraction of the population in the corresponding compartment.

We represent the environment with n, which is a linear transformation of the fraction of infected,

$$n(i) = n_0 - \epsilon i \tag{1}$$

where $n_0 \in [0,1]$ and $\epsilon > 0$ are constants. The constant n_0 is the risk perception of the population when there is no infection ($i = 0$). The constant ϵ is the rate of decrease in the environment state per increase in the fraction of infected. In a sense, ϵ measures the sensitivity of the public to changes in the case numbers. Throughout the paper, we choose n_0 and ϵ such that $n(i) \geq 0$ for all i values. Note that when $n_0 = 1$ and $\epsilon = 1$, $n(0) \in [0,1]$ since $i \in [0,1]$.

The current state of the environment determines the incentives of individuals captured by a symmetric 2×2 game where the strategies are cooperation ($\mathcal{C}$) and defection ($\mathcal{D}$), and the payoff is given by

$$A_n = (1-n)\begin{bmatrix} R_0 & S_0 \\ T_0 & P_0 \end{bmatrix} + n\begin{bmatrix} R_1 & S_1 \\ T_1 & P_1 \end{bmatrix}. \tag{2}$$

The payoff above is a convex combination of two games. When the environment is bad, the game payoffs are given by the first matrix A_0 above. When the environment is good, the game payoffs are given by the second matrix A_1 above. As per (1) and the fact that $i = 0$ is the good environment, the payoff matrix when the environment is given by A_{n_0} with elements defined as $R_{n_0} = (1-n_0)R_0 + n_0 R_1$, $S_{n_0} = (1-n_0)S_0 + n_0 S_1$, $T_{n_0} = (1-n_0)T_0 + n_0 T_1$, and $P_{n_0} = (1-n_0)P_0 + n_0 P_1$. In the good-environment, we assume $R_{n_0} < T_{n_0}$ and $S_{n_0} < P_{n_0}$ which ensures that defection from taking the recommended public health measures is a dominant strategy. We will refer to A_{n_0} or A_1 as the prisoner's dilemma game. We do not impose any restrictions on the payoffs in the bad-environment game A_0.

Given the game A_n, the payoffs of a cooperator and a defector in a population with $x \in [0,1]$ fraction of cooperators are respectively given by

$$f_{\mathcal{C}}(x,n) = R_n x + S_n(1-x), \text{ and} \tag{3}$$

$$f_{\mathcal{D}}(x,n) = T_n x + P_n(1-x), \tag{4}$$

where R_n, S_n, T_n, and P_n are as previously defined for any environment value $n \in [0,1]$. We assume the fraction of

cooperators in the population evolve according to replicator dynamics [23],

$$\dot{x} = x(1-x)(f_{\mathcal{C}}(x,n) - f_{\mathcal{D}}(x,n)). \tag{5}$$

According to the replicator dynamics, the fraction of cooperators increases if the payoff of a cooperator is larger than the payoff of a defector, i.e., if $f_{\mathcal{C}}(x,n) > f_{\mathcal{D}}(x,n)$. Through the dependence of n on the disease prevalence i in (1), the fraction of cooperators depend on the state of the disease.

The fraction of cooperators x captures the ratio of individuals complying with the recommended public health measures, i.e., social distancing, in the population. The modified SEIRS dynamics with social distancing behavior is as follows

$$\dot{s} = -\beta(1-x)\cdot i \cdot s + \mu \cdot r, \tag{6}$$
$$\dot{e} = \beta(1-x)\cdot i \cdot s - \eta \cdot e, \tag{7}$$
$$\dot{i} = \eta \cdot e - \alpha \cdot i, \tag{8}$$
$$\dot{r} = \alpha \cdot i - \mu \cdot r, \tag{9}$$

where β, η, α, and μ are disease specific positive valued parameters respectively representing the rate of infection, incubation, healing, and immunity loss. In (6), an increase in the frequency of cooperators x reduces the transmission rate. This reduction in turn leads to a reduction in the infection level, which means a better environment. A better environment changes the payoffs moving the payoffs closer to A_1 in which the defection is a dominant strategy. The constants n_0 and ϵ in (1) determine how close the game gets to A_1 and how fast the game approaches A_0 as a function of the ratio of infected in the population, respectively. We analyze the equilibria of the dynamics (5)-(9) and the emerging dynamics with respect to these parameters next.

III. Equilibria of SEIRS dynamics with social distancing

The feasible region of the dynamics in (5)-(9) is $\Delta = \{(e,i,r,x) \in \mathbb{R}^4_+ | 0 \le e+i+r \le 1, 0 \le x \le 1\}$, which is positively invariant, i.e., given any non-negative initial solution in Δ, the dynamics remain in Δ. We note here that $s(t)+e(t)+i(t)+r(t) = 1$ for all $t \ge 0$ and the dynamics in (6) is redundant. We restrict our analysis to the Δ region.

A. Disease-free equilibria (DFE)

The population is disease free when $e(t)+i(t) = 0$ for all $t \ge 0$. In the disease free setting where $i = 0$, there are three values that make $\dot{x} = 0$ in (5) are $\{0, x_{int}, 1\}$ where

$$x_{int} = \frac{P_{n_0} - S_{n_0}}{R_{n_0} - T_{n_0} + (P_{n_0} - S_{n_0})} \tag{10}$$

is obtained by finding the value of x such that $f_{\mathcal{C}}(x,n_0) - f_{\mathcal{D}}(x,n_0) = 0$ in (5). Note that when $i = 0$, we have $n = n_0$ by (1). Based on the assumption that A_{n_0} is a prisoner's dilemma game ($R_{n_0} < T_{n_0}$ and $S_{n_0} < P_{n_0}$), we have either $x_{int} > 1$ or $x_{int} < 0$. Thus, the interior equilibrium x_{int} does not exist. Accordingly, we have the following disease free equilibria $\mathbf{p}_0 := (e=0, i=0, r=0, x=0)$ and $\mathbf{p}_1 := (e=0, i=0, r=0, x=1)$. Next, we analyze the stability of the two equilibria.

Lemma 1 *Consider the two DFE $\mathbf{p}_0$ and $\mathbf{p}_1$. If $\beta - \alpha < 0$, then $\mathbf{p}_0$ is locally stable. The equilibrium $\mathbf{p}_1$ is not stable.*

Proof: The Jacobian matrix of (5)-(9) at an arbitrary point $\mathbf{p} = (e,i,r,x)$ is given by

$$J(\mathbf{p}) = \begin{pmatrix} -\eta & \beta(1-x)s & 0 & -\beta i s \\ \eta & -\alpha & 0 & 0 \\ 0 & \alpha & -\mu & 0 \\ 0 & \frac{\partial h(x,n)}{\partial i} & 0 & \frac{\partial h(x,n)}{\partial x} \end{pmatrix} \tag{11}$$

where $s = 1-e-i-r$, and we define $h(x,n)$ as the replicator dynamics in (5) to simplify exposition. At point $\mathbf{p} = \mathbf{p}_0$, we have $\frac{\partial h(x,n)}{\partial i}|_{\mathbf{p}_0} = 0$ and $\frac{\partial h(x,n)}{\partial x}|_{\mathbf{p}_0} = f_{\mathcal{C}}(0,n_0) - f_{\mathcal{D}}(0,n_0)$. The characteristic equation at $\mathbf{p}_0$ is given by

$$(\lambda+\mu)(P_{n_0} - S_{n_0} + \lambda)((\eta+\lambda)(\alpha+\lambda) - \beta\eta) = 0 \tag{12}$$

When $\beta - \alpha < 0$, all the solutions to the above equation have negative real parts.

At point $\mathbf{p} = \mathbf{p}_1$, we have $\frac{\partial h(x,n)}{\partial i}|_{\mathbf{p}_1} = 0$ and $\frac{\partial h(x,n)}{\partial x}|_{\mathbf{p}_1} = -f_{\mathcal{C}}(1,n_0) + f_{\mathcal{D}}(1,n_0)$. Then the characteristic equation at $\mathbf{p}_1$ is given by

$$(\lambda+\mu)(S_{n_0} - P_{n_0} + \lambda)(\eta+\lambda)(\alpha+\lambda) = 0 \tag{13}$$

which has a positive solution, $\lambda = P_{n_0} - S_{n_0} > 0$. Thus $\mathbf{p}_1$ is not stable. ■

According to the model, the disease spread can completely stop if the fraction of cooperators in the population is 1 ($x = 1$). The above result shows that this equilibrium point $\mathbf{p}_1$ is unstable. The reason for the instability of $\mathbf{p}_1$ is the replicator dynamics, and the assumption that the defection is the dominant strategy in the good environment. Despite the instability of $\mathbf{p}_1$, the disease-free states ($e = 0$ and $i = 0$) is asymptotically stable if $\beta - \alpha < 0$ as we state next.

Lemma 2 *If $\beta - \alpha < 0$, then the disease free manifold $D_f = \{\mathbf{p} \in \Delta | e+i = 0\}$ is globally asymptotically stable.*

Proof : The set D_f is positively invariant. Consider the Lyapunov function $V = e+i$ where $V > 0$ for any $e+i > 0$ and $V = 0$ for all $\mathbf{p} \in D_f$. Differentiating V along the dynamics, we get

$$\dot{V} = \dot{e} + \dot{i} = \alpha i\big(\frac{\beta}{\alpha}(1-x)s - 1\big) \tag{14}$$

where $s = 1-e-i-r$. Given the assumption, we have $\dot{V} < 0$ for all $\mathbf{p} \in \Delta \setminus D_f$. Moreover, $\dot{V}(\mathbf{p}) = 0$ when $\mathbf{p} \in D_f$ since $i = 0$. Thus, the global asymptotic stability follows by La Salle's invariance principle. ■

The above result implies that if the inherent disease dynamics is such that the disease will be eradicated, i.e., $\beta - \alpha < 0$, the behavior dynamics do not affect the stability of the disease free state.

B. Disease-free equilibrium in the absence of loss of immunity

We consider SEIR dynamics where $\mu = 0$ in (6)-(9). In this setting, we cannot have a sustained epidemic, i.e., $i(\infty) = 0$. Still, a large fraction of the population can be infected by the time the disease disappears. In this setting, we care whether the disease will invade or die out quickly. Considering the change in $e + i$ in (14), we have that the exposed and infectious individuals will decay exponentially if there exists a time t_0 such that $\beta(1 - x(t_0))s(t_0) < \alpha$ for $t \geq t_0$. If $\beta(1 - x(t_0))s(t_0) > \alpha$ at time t_0, the disease will grow exponentially around time t_0. If $\beta < \alpha$, we have that $\beta(1 - x) < \alpha$ for any $x \in [0, 1]$. Thus, the disease will exponentially decrease for any initial condition x and s if $\beta < \alpha$ [24].

If $\beta > \alpha$, then for initial conditions where $x \approx 0$ and $s \approx 1$, the disease will grow exponentially. In this setting, the population reaches *herd immunity* when $s(t) = \alpha/\beta$. After herd immunity is reached, the fraction of exposed and infected individuals will exponentially decrease to zero regardless of the social distancing actions in the population.

C. Endemic equilibria

In this section, we characterize the fraction of individuals in each compartment when the disease is endemic, i.e., $e(\infty) > 0$ and $i(\infty) > 0$.

Lemma 3 *Suppose $\beta - \alpha > 0$. We have the following endemic equilibrium under full defection, i.e., $x^* = 0$,*

$$s^* = \frac{\alpha}{\beta}, e^* = \frac{\alpha}{\eta} i^*,\ i^* = (1 - \frac{\alpha}{\beta})c_0,\ r^* = \frac{\alpha}{\mu} i^*, \qquad (15)$$

where $c_0 := \frac{\eta\mu}{\eta\mu + \alpha\mu + \alpha\eta}$.

The proof follows by letting $x^* = 0$ and solving for the s, e, i, r values that make the right hand side of the SEIRS dynamics in (6)-(9) equal to zero. In this endemic equilibrium, the behavior has no effect since all individuals are defecting. Indeed, we recover the standard SEIRS model where the endemic equilibrium (15) is stable when $\beta - \alpha > 0$.

When the population is fully cooperating, i.e., when $x^* = 1$, there does not exist an endemic equilibrium, which means the disease will be eradicated. Next, we focus on the interior fixed point of the replicator dynamics that satisfy $f_{\mathcal{C}}(x, n) - f_{\mathcal{D}}(x, n) = 0$. For a given $x \in (0, 1)$, we have the environment value that makes $f_{\mathcal{C}}(x, n_{int}) - f_{\mathcal{D}}(x, n_{int}) = 0$ as follows,

$$n_{int} = \frac{(1 - x)\delta_{SP_0} + x\delta_{RT_0}}{(1 - x)(\delta_{PS_1} + \delta_{SP_0}) + x(\delta_{TR_1} + \delta_{RT_0})} \qquad (16)$$

where $\delta_{SP_0} = S_0 - P_0$, $\delta_{RT_0} = R_0 - T_0$, $\delta_{PS_1} = P_1 - S_1$ and $\delta_{TR_1} = T_1 - R_1$. Given the n_{int} value, we have the following set of equations that is satisfied by an endemic equilibrium,

$$i = \frac{n_0 - n_{int}}{\epsilon},\ e = \frac{\alpha}{\eta} i,\ r = \frac{\alpha}{\mu} i,\ s = 1 - c_0 i, \qquad (17)$$

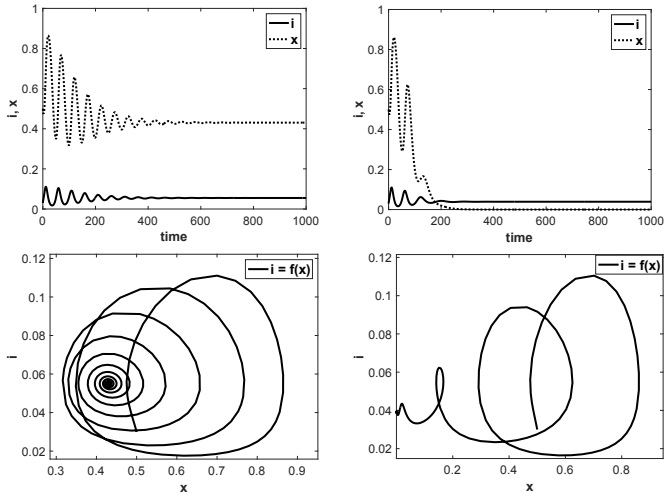

$\mu = 1/45$ days^{-1} $\mu = 1/90$ days^{-1}

Fig. 2. Sustained oscillations and stable endemic equilibrium with loss of immunity (Left) $\mu = 1/45$ and (Right) $\mu = 1/90$. Top figures shows infection ratio i and cooperation frequency x values over time. Bottom figures show the phase plot of i and x. Payoff and disease parameters, and initial conditions are as follows: $A_0 = \begin{bmatrix} 3.5 & 1 \\ 2 & 0.25 \end{bmatrix}$, $A_1 = \begin{bmatrix} 0.5 & 1 \\ 1 & 1.25 \end{bmatrix}$, $n_0 = 0.8, \epsilon = 2, \beta/\alpha = 4, \eta = 1, s(0) = 0.95, e(0) = 0.02, i(0) = 0.03, r(0) = 0, x(0) = 0.5$. Starting from near equilibrium levels in i and x, the oscillations grow and then decline before converging to the endemic infection levels. The interior equilibrium of cooperation frequency becomes stable at a faster loss of immunity (compare left and right).

where c_0 is as defined in Lemma 3. We have the fraction of cooperators given by

$$x = 1 - \frac{\alpha}{\beta}\frac{1}{s}. \qquad (18)$$

In the above equations we expressed e, r, and s in terms of i which is written in terms of n_{int} given in (16). From the equations in (17), we can solve for x in (18) after substituting i into the equation for s, and then substituting the right hand side of the equation for s into (18) to get,

$$x = 1 - \frac{\alpha}{\beta}\frac{\epsilon}{\epsilon - c_o(n_0 - n_{int})} \qquad (19)$$

where n_{int} is given in (16). In the general case, the equation above leads to a quadratic equation. Below we characterize the endemic equilibrium for a specific class of payoffs.

Lemma 4 *Consider the following payoff matrix at a given n value*

$$A_n = (1 - n)\begin{bmatrix} T & P \\ R & S \end{bmatrix} + n\begin{bmatrix} R & S \\ T & P \end{bmatrix}. \qquad (20)$$

where $R > S$, and $T > P$. Assume $\beta - \alpha > 0$ and $n_0 > 0.5$, then the endemic equilibrium is as follows,

$$s^* = \frac{\epsilon - c_0(n_0 - 0.5)}{\epsilon},\ e^* = \frac{\alpha}{\eta} i^*,\ i^* = \frac{n_0 - 0.5}{\epsilon},\ r^* = \frac{\alpha}{\mu} i^* \qquad (21)$$

and $x^* = 1 - \frac{\alpha}{\beta}\frac{\epsilon}{\epsilon - c_o(n_0 - 0.5)}$ with constant $c_0 := \frac{\eta\mu}{\eta\mu + \alpha\mu + \alpha\eta}$.

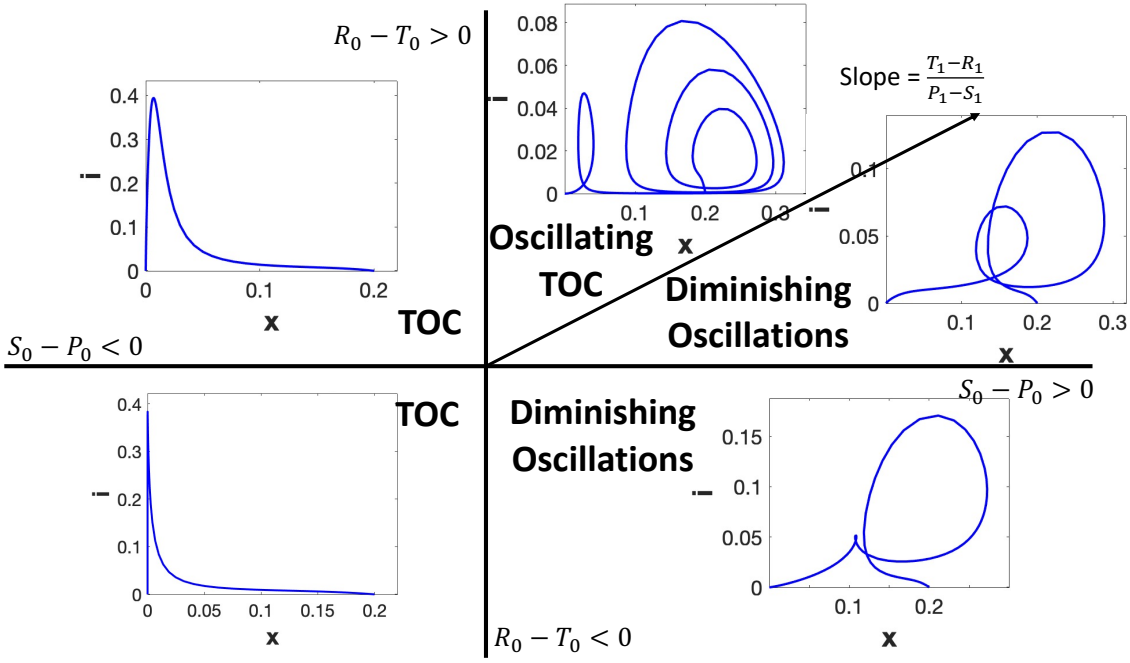

Fig. 3. Summary of the dynamics given all possible combinations of payoff matrix values in a bad environment. The plots inside each region show a characteristic phase plot between i and x for the corresponding payoff matrix values. Payoff and disease parameters, and initial conditions are as follows: $A_1 = \begin{bmatrix} 0.5 & 1 \\ 1 & 1.25 \end{bmatrix}, \epsilon = 2, n_0 = 0.8, s(0) = 0.99, e(0) = 0.01, i(0) = 0, r(0) = 0, x(0) = 0.7, \beta/\alpha = 5, \mu = 0, \eta = 1$. From the Oscillating TOC moving counter clockwise, these matrices are: $\begin{bmatrix} 3.9 & 1 \\ 2 & 0.25 \end{bmatrix}, \begin{bmatrix} 2.7 & 1 \\ 2 & 1.25 \end{bmatrix}, \begin{bmatrix} 3 & 1 \\ 3.2 & 1.25 \end{bmatrix}, \begin{bmatrix} 3 & 1 \\ 3.2 & 0.25 \end{bmatrix}, \begin{bmatrix} 2.5 & 1 \\ 2 & 0.25 \end{bmatrix}$. The number of oscillations increase as the strength of selection for cooperators in replicator dynamics increases, eventually yielding growing oscillations.

Proof: Given the payoffs in (20), we have that $n_{int} = 0.5$ for any x value. The relations in (21) follow from the equations in (17) when we plug in $n_{int} = 0.5$. ■

The specific class of games, we consider has a form of symmetry such that cooperation is a Nash equilibrium when $n = 0$, and defection is a Nash equilibrium when $n = 1$. Moreover, the embedded symmetry makes sure that $n_{int} = 1/2$ regardless of the value of x. We see the effect of the rate of decrease in the environment state ϵ on the endemic equilibrium levels. When ϵ is larger, there is a larger change in the payoffs per unit change in the fraction of infected. That is, the population responds stronger to the change in the fraction of infected. According to the endemic equilibrium in (21), a larger ϵ leads to smaller fraction of exposed and infected, and thus a larger fraction of susceptible individuals.

The symmetry in the payoffs in (19) also makes sure that the swing from cooperation dominant to defection dominant payoffs is at the 'right balance' to induce another wave of infections. Indeed, when the ratio $(T_1 - R_1)/(P_1 - S_1)$ is equal to $(R_0 - T_0)/(S_0 - P_0)$, periodic oscillations around the interior equilibrium are observed in the coupled evolutionary dynamics considered in [9]. In [9], the environmental dynamics is a first-order differential equation that increases with enough cooperators and otherwise depletes. Here, we observe a similar phenomenon of sustained oscillations when the environment dynamics follow (8) in an SEIRS model—see Fig. 2. The payoff parameters in Fig. 2 are such that $(T_1 - R_1)/(P_1 - S_1) = (R_0 - T_0)/(S_0 - P_0)$. Moreover, observe that as the average loss of immunity increases from $\mu = 1/45$ to $\mu = 1/90$, the interior equilibrium $x^* > 0$ is no longer stable.

IV. Multiple Peaks Until Herd Immunity in the Absence of Loss of Immunity

The loss of immunity is at least 6 months in COVID-19 infections barring new variant introductions, meaning that μ is much smaller than the values considered in Fig. 2. In this section, we characterize the trajectories of i and x when loss of immunity is ignored ($\mu = 0$) under general payoff matrix values for the bad environment state, i.e., A_0.

There are four cases considering relative values of R_0 and T_0, and P_0 and S_0 that may affect the game type and the evolutionary dynamics. First, A_0 is an anti-coordination game when $R_0 < T_0$ and $S_0 > P_0$. In an anti-coordination game, there exists a mixed Nash equilibrium, i.e., an interior fixed point of the replicator dynamics in the form given in (10) replacing n_0 with 0. Second, A_0 is a coordination game with $R_0 > T_0$ and $S_0 < P_0$. The coordination game also has a mixed Nash equilibrium, i.e., an interior fixed point of the replicator dynamics in the form given in (10) replacing n_0 with 0. The mixed Nash equilibrium is unstable under replicator dynamics. In the third case, we have cooperation dominant game when $R_0 > T_0$ and $S_0 > P_0$. The fourth scenario is the defection dominant setting with $R_0 < T_0$ and $S_0 < P_0$.

We summarize the characteristic dynamics of each region

in Fig. 3. We note here that we do not consider loss of immunity, i.e., $\mu = 0$, thus the disease eventually reaches an exponential decline phase once herd immunity is reached in all the scenarios as per the discussion in Section III-B. In the coordination and defection dominant scenarios for A_0, we observe that there is a single peak, and the population defects starting from $x(0) > 0$—see the tragedy of the commons (TOC) in top-left and bottom-left quadrants of Figure 3. The defection is faster when the game is defection dominant. In the event that A_0 is an anti-coordination game, we observe a response from the public in increasing the fraction of cooperators when the number of the cases i increases. This response leads to diminishing oscillations in the number of cases. However, the increase in the cooperator frequency is not strong enough to induce multiple oscillations before herd immunity is reached—see Figure 3 bottom-right quadrant. In the cooperation dominant case, the increase in cooperator frequency is stronger leading to multiple diminishing oscillations in the region where

$$\frac{T_1 - R_1}{P_1 - S_1} > \frac{R_0 - T_0}{S_0 - P_0}. \tag{22}$$

Note that in Fig. 2, we analyzed the same case in which the above relation is satisfied with an equality when the loss of immunity exists. There, the system converged to an endemic equilibrium after growing and then declining oscillations. Coincidentally, when the inequality above is reversed, we observe growing oscillations until herd immunity is reached—see Fig. 3 top-right. As in [9], we term this phenomenon as oscillating tragedy of the commons (oscillating TOC).

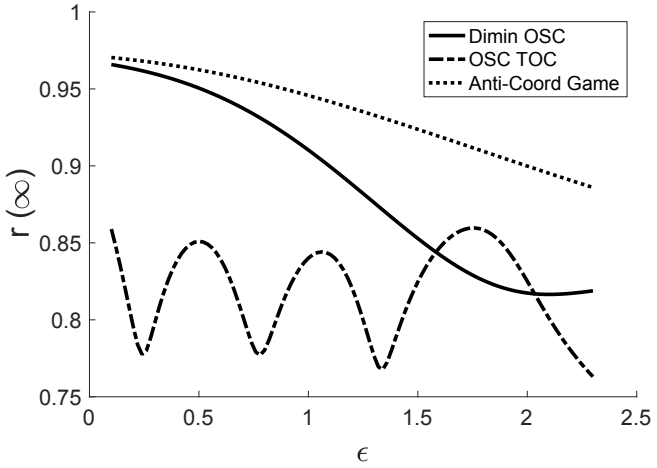

Fig. 4. Total outbreak size in different regions as a function of the sensitivity parameter to changes in number of cases ϵ. Payoff and disease parameters, and initial conditions are as follows: $n_0 = 0.8, \beta/\alpha = 4, \mu = 0, \eta = 1, s(0) = 0.99, e(0) = 0.01, i(0) = 0, r(0) = 0, x(0) = 0.7$. $A_1 = \begin{bmatrix} 0.5 & 1 \\ 1 & 1.25 \end{bmatrix}$. The value of the matrix A_0 for the Dimin OSC, OSC TOC, and Anti-coordination game is $\begin{bmatrix} 2.5 & 1 \\ 2 & 0.25 \end{bmatrix}$, $\begin{bmatrix} 3.9 & 1 \\ 2 & 0.25 \end{bmatrix}$, $\begin{bmatrix} 3 & 1 \\ 3.2 & 0.25 \end{bmatrix}$, respectively. As the sensitivity parameter increases, the outbreak size tends to decrease.

Besides exhibiting oscillations, the strong response to disease prevalence leads to a reduction in the total outbreak

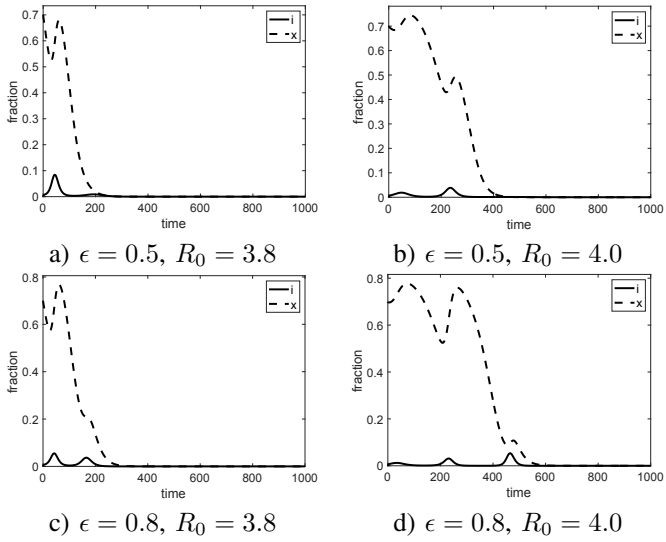

Fig. 5. Multiple diminishing and growing oscillations as a function the sensitivity parameter ϵ and reward at bad environment state R_0. Payoff and disease parameters, and initial conditions are as follows: $A_0 = \begin{bmatrix} R_0 & 1 \\ 2 & 0.2 \end{bmatrix}$, $A_1 = \begin{bmatrix} 0.5 & 1 \\ 1 & 1.25 \end{bmatrix}$, $n_0 = 0.8, \beta/\alpha = 4, \eta = 1, s(0) = 0.99, e(0) = 0.01, i(0) = 0, r(0) = 0, x(0) = 0.7$. (Left) $R_0 = 3.8$ corresponds to diminishing oscillations scenario. (Right) $R_0 = 4.0$ corresponds to oscillating TOC scenario. Increasing sensitivity parameter ϵ from 0.5 (Top) to 0.8 (Bottom), less severe but higher number of peaks are observed.

size, defined as the cumulative number of infected, i.e., $r(\infty)$. Fig. 4 shows the outbreak size in different regions as a function of the strength of change in the environment with respect to i, i.e., ϵ. As ϵ increases, the payoffs change faster with changes to the case numbers. Here, the general trend is that the outbreak size decreases as the public becomes more sensitive to the fraction of infected, i.e., as ϵ increases. However, the decrease in the outbreak size is not monotonic, especially for the oscillating TOC region. This is because oscillations grow faster as ϵ increases. In such a setting, the outbreak size depends largely on where the oscillations are when the herd immunity is reached. For instance, if the fraction of cooperators is relatively large when herd immunity is reached, the outbreak size tends to be smaller.

The time to reach herd immunity depends on the size of the peaks. In standard epidemic models without social distancing, the number of cases decreases exponentially after the peak in number of cases is reached. Intuitively, when the public social distancing behavior changes fast with respect to the disease prevalence, we would expect to observe larger number of lower peaks. This is because the disease would be suppressed by the increasing frequency of cooperators early, which then would remain a large number of the population susceptible in the next surge. Comparing different ϵ values in Figs. 5 (a) and (c) or (b) and (d), we have larger number of lower peaks in (c) or (d) when ϵ is larger, which confirms this intuition. Similarly, when the reward from cooperation in the bad environment (R_0) increases, the selection strength for cooperators is larger in bad state, suppressing the peak sizes. Comparing Figs. 5 (a) and (b) or (c) and (d), we see

that peaks of the case counts are smaller when R_0 is larger.

V. Conclusions

We proposed a disease spread model with an evolutionary social distancing response to disease prevalence. The current state of the disease determined the payoffs of individuals in the society. We used evolutionary game theory to model the change in compliance of individuals to the recommended public health measures. The behavior of individuals determined the transmission rate of the disease regulating the flow of individuals from a susceptible to an exposed state in the SEIRS model. By focusing on game payoffs, we identified disease trajectories where multiple growing peaks are observed before herd immunity is reached when there is no loss of immunity. Moreover, when the loss of immunity was small, we observed growing and then decreasing oscillations around the endemic equilibrium levels of the disease. Together these results seek to understand human behavior related mechanisms that may be driving the multiple peaks and oscillations observed during infectious disease outbreaks. Lastly, the model provides a framework for estimating the public's evaluation of the cost and benefits of social distancing measures using publicly available data, e.g., hospitalizations or morbidity numbers. Quantifying public's inclination to adhere to public health recommendations can be used in forecasting disease trajectory or can aid in public health communication campaigns.

References

[1] D. J. Bregman and A. D. Langmuir, "Farr's law applied to aids projections," *Jama*, vol. 263, no. 11, pp. 1522–1525, 1990.

[2] K. Leung, J. T. Wu, D. Liu, and G. M. Leung, "First-wave COVID-19 transmissibility and severity in China outside Hubei after control measures, and second-wave scenario planning: a modelling impact assessment," *The Lancet*, vol. 395, no. 10233, pp. 1382–1393, 2020.

[3] R. M. Anderson and R. M. May, *Infectious diseases of humans: dynamics and control*. Oxford university press, 1992.

[4] C. Nowzari, V. M. Preciado, and G. J. Pappas, "Analysis and control of epidemics: A survey of spreading processes on complex networks," *IEEE Control Systems Magazine*, vol. 36, no. 1, pp. 26–46, 2016.

[5] P. E. Paré, C. L. Beck, and T. Başar, "Modeling, estimation, and analysis of epidemics over networks: An overview," *Annual Reviews in Control*, 2020.

[6] M. U. Kraemer, C.-H. Yang, B. Gutierrez, C.-H. Wu, B. Klein, D. M. Pigott, L. Du Plessis, N. R. Faria, R. Li, W. P. Hanage *et al.*, "The effect of human mobility and control measures on the COVID-19 epidemic in China," *Science*, vol. 368, no. 6490, pp. 493–497, 2020.

[7] R. West, S. Michie, G. J. Rubin, and R. Amlôt, "Applying principles of behaviour change to reduce SARS-CoV-2 transmission," *Nature Human Behaviour*, vol. 4, no. 5, pp. 451–459, 2020.

[8] O. N. Bjørnstad, K. Shea, M. Krzywinski, and N. S. Altman, "The SEIRS model for infectious disease dynamics," *Nature methods*, vol. 17, no. 6, pp. 557–558, 2020.

[9] J. S. Weitz, C. Eksin, K. Paarporn, S. P. Brown, and W. C. Ratcliff, "An oscillating tragedy of the commons in replicator dynamics with game-environment feedback," *Proceedings of the National Academy of Sciences*, vol. 113, no. 47, pp. E7518–E7525, 2016. [Online]. Available: https://www.pnas.org/content/113/47/E7518

[10] A. R. Tilman, J. B. Plotkin, and E. Akçay, "Evolutionary games with environmental feedbacks," *Nature communications*, vol. 11, no. 1, pp. 1–11, 2020.

[11] G. Hardin, "The tragedy of the commons," *Journal of Natural Resources Policy Research*, vol. 1, no. 3, pp. 243–253, 2009.

[12] S. Funk, M. Salathé, and V. A. Jansen, "Modelling the influence of human behaviour on the spread of infectious diseases: a review," *Journal of the Royal Society Interface*, vol. 7, no. 50, pp. 1247–1256, 2010.

[13] T. C. Reluga, "Game theory of social distancing in response to an epidemic," *PLoS Comput Biol*, vol. 6, no. 5, p. e1000793, 2010.

[14] G. Theodorakopoulos, J.-Y. Le Boudec, and J. S. Baras, "Selfish response to epidemic propagation," *IEEE Transactions on Automatic Control*, vol. 58, no. 2, pp. 363–376, 2012.

[15] K. Paarporn, C. Eksin, J. S. Weitz, and J. S. Shamma, "The effect of awareness on networked SIS epidemics," in *2016 IEEE 55th Conference on Decision and Control (CDC)*. IEEE, 2016, pp. 973–978.

[16] C. Eksin, J. S. Shamma, and J. S. Weitz, "Disease dynamics in a stochastic network game: a little empathy goes a long way in averting outbreaks," *Scientific reports*, vol. 7, no. 1, pp. 1–13, 2017.

[17] J. S. Weitz, S. W. Park, C. Eksin, and J. Dushoff, "Awareness-driven behavior changes can shift the shape of epidemics away from peaks and toward plateaus, shoulders, and oscillations," *Proceedings of the National Academy of Sciences*, vol. 117, no. 51, pp. 32 764–32 771, 2020.

[18] A. R. Hota, T. Sneh, and K. Gupta, "Impacts of game-theoretic activation on epidemic spread over dynamical networks," *arXiv preprint arXiv:2011.00445*, 2020.

[19] A. Glaubitz and F. Fu, "Oscillatory dynamics in the dilemma of social distancing," *Proceedings of the Royal Society A*, vol. 476, no. 2243, p. 20200686, 2020.

[20] M. Ye, L. Zino, A. Rizzo, and M. Cao, "Modelling collective decision-making during epidemics," *arXiv preprint arXiv:2008.01971*, 2020.

[21] P. Poletti, M. Ajelli, and S. Merler, "The effect of risk perception on the 2009 H1N1 pandemic influenza dynamics," *PloS one*, vol. 6, no. 2, p. e16460, 2011.

[22] M. A. Amaral, M. M. de Oliveira, and M. A. Javarone, "An epidemiological model with voluntary quarantine strategies governed by evolutionary game dynamics," *Chaos, Solitons & Fractals*, vol. 143, p. 110616, 2021.

[23] J. Hofbauer, K. Sigmund *et al.*, *Evolutionary games and population dynamics*. Cambridge university press, 1998.

[24] J. Ma and Z. Ma, "Epidemic threshold conditions for seasonally forced SEIR models," *Mathematical Biosciences & Engineering*, vol. 3, no. 1, p. 161, 2006.